

¹³C NMR Studies of Vitamin C Transport and Its Redox Cycling in Human Erythrocytes[†]

Uwe Himmelreich,[‡] Kenneth N. Drew,[§] Anthony S. Serianni,[§] and Philip W. Kuchel^{*,‡}

Department of Biochemistry, University of Sydney, NSW 2006, Australia, and Department of Chemistry and Biochemistry, College of Science, University of Notre Dame, Notre Dame, Indiana 46556

Received April 1, 1997; Revised Manuscript Received February 23, 1998

ABSTRACT: ¹³C NMR spectra of labeled [1-¹³C]- and [2-¹³C]ascorbic acid were seen to contain resonances arising from the intra- and extracellular populations in suspensions of human erythrocytes; i.e., they displayed the “split-peak” phenomenon. This new observation enabled the ready determination of the location, whether inside or outside cells, of the redox reactions in which the vitamin C was involved and to monitor the transport of the compounds into and out of the cells. Thus, the membrane permeability of ascorbic acid and the apparent V_{\max} and K_M for the reduction of dehydroascorbic acid were determined in a noninvasive manner. In contrast to other work, evidence was found of a transporter of dehydroascorbic acid which is different from the glucose transporter. This transport system also appeared to be involved in the simultaneous reduction of dehydroascorbic acid on its passage into the cells. A second reduction process appeared to occur extracellularly, by the passage of reducing equivalents through the plasma membrane, as occurs with the reduction of ferricyanide. Evidence is presented that the processes of vitamin C recycling rely on different cellular sources of reducing equivalents. Whereas the transport and reduction via the membrane appeared to be dependent on glycolysis (NADH), the reduction of intracellular dehydroascorbic acid, formed in the process of transmembrane electron transfer or by transport from the outside of the cell, is currently thought to depend on NADPH.

Vitamin C is involved in several different cell-physiological functions in all living organisms, and it is an essential nutrient for species such as humans who lack its synthetic pathway (1). Although vitamin C is critical to human cell functions, especially in the response of cells to oxidative stress, the details of how the chemically unstable oxidized dehydroascorbic acid (DHAA)¹ becomes re-reduced to the more stable ascorbic acid (AA) are not clear. This process of vitamin C redox cycling may add to the antioxidant potential of cells, since, for example, even low concentrations of AA enhance the rate at which human red blood cells (RBCs) respond to extracellular oxidative agents (2–4).

Several authors argue that the reduction of DHAA may take place on the membrane surface (3, 5, 6), or inside the RBC (2, 7). The question arises whether DHAA must be taken up by the RBC to become reduced to AA or whether the transport and subsequent reduction are processes that are both localized on or in the RBC membrane. Furthermore,

it is not entirely clear how AA contributes to the antioxidant potential of RBCs, if it has to be released by the cell to transfer reducing equivalents to sources of extracellular oxidative stress, or if it acts as an electron donor to a transmembrane oxidoreductase (3, 8, 9).

Evidence for intracellular recycling of vitamin C was supported by results obtained from Basu et al. (10). They found that DHAA reduction was carried out by intracellular reduced glutathione (GSH) that does not cross the RBC membrane. However, this is in contrast to results which indicate the involvement of a transmembrane oxidoreductase (8).

It is known that DHAA is transported much more rapidly into RBCs than AA (7, 11, 12). There is controversy, however, regarding the pathway of vitamin C transport into the RBC. Some observations have linked the transport of DHAA with hexose transport systems in mammalian cells (8, 11, 13), whereas others argue that DHAA enters and leaves the RBC by simple diffusion (14) or via a glucose-independent system for DHAA transport in RBCs, which is postulated to be a facilitated diffusion pathway (15). On the other hand, AA is thought to enter and leave the RBC by simple diffusion (7, 16) or by the GLUT1 glucose transporter (8).

The lack of agreement among various contemporary studies concerning vitamin C transport may be due, at least in part, to its chemical instability, especially of DHAA, and to a great extent on the limitations of the analytical methods used for measuring vitamin C concentrations (14, 17). These

[†] This work was funded by a project grant to P.W.K. from the Australian NH&MRC. U.H. is grateful for the award of a Deutsche Forschungsgemeinschaft (DFG) Fellowship.

* Address correspondence to this author.

[‡] University of Sydney.

[§] University of Notre Dame.

¹ Abbreviations: AA, ascorbic acid, ascorbate; CNDB, 1-chloro-2,4-dinitrobenzene; DHAA, dehydroascorbic acid, dehydroascorbate; DKG, diketogulonic acid; DMMP, dimethyl methylphosphonate; DNDS, dinitrostilbene-2,2'-disulfonate; GSH, reduced glutathione; GSSG, oxidized glutathione; NMR, nuclear magnetic resonance; PBS, phosphate-buffered saline; *p*-CMPS, *p*-chloromercuriphenylsulfonate; RBC(s), red blood cell(s), erythrocyte(s).

analytical difficulties were surmounted in the present work by using ^{13}C NMR spectroscopy to monitor the processes of transport and redox recycling of vitamin C in RBCs in vitro, in a noninvasive and continuous manner; AA, DHAA, and degradation products could be detected simultaneously.

The only previous estimate of the rate of AA regeneration was obtained indirectly from the rate of ascorbate-dependent ferricyanide reduction, but this may be influenced by many other factors (8).

The only apparent drawback of using ^{13}C NMR, as in the present work, is the necessity to perform the experiments at DHAA concentrations higher than encountered in vivo, to achieve acceptable signal-to-noise ratios in the spectra.

MATERIALS AND METHODS

Erythrocyte Preparations. Venous blood was obtained by venipuncture from five different healthy volunteers. The responses (i.e., the rate of reduction of ferricyanide) of their RBCs to oxidative stress brought about by extracellular ferricyanide in the presence and absence of vitamin C were similar (see ref 4). The RBCs were usually used within 48 h after collection. The blood was diluted into 3 vol of phosphate-buffered saline [PBS; 10 mM ($\text{Na}_2\text{HPO}_4/\text{NaH}_2\text{PO}_4$), 3 mM KCl, 1 mM KH_2PO_4 , 0.6 mM MgSO_4 , 0.6 mM MgCl_2 , and 140 mM NaCl] and then centrifuged (3000g, 5 min, 4 °C). Because the uptake of AA by leukocytes is ~40 times more rapid than by RBCs (13), the plasma, the buffy coat, and the uppermost RBC layers were carefully removed by aspiration. The final ratio of RBCs to leukocytes for the washed and filtered cells was always greater than 5000:1. The washing and centrifugation steps were carried out three times. Cells were stored before use for up to 48 h in PBS containing 5 mM glucose at 4 °C. Finally, the cells were gassed with CO to convert oxy- and deoxyhemoglobin to carbonmonoxyhemoglobin, whose stable diamagnetic nature ensures maximum resolution in the NMR spectra (18, 19).

Packed cells were suspended in a PBS solution containing 5 mM glucose (osmolality, 290 mOsmol kg^{-1} ; pH 7.0 at 25 °C) before the NMR experiments were begun. The hematocrits (H_c) were usually adjusted to 0.5–0.7. Control measurements were also performed with lower and higher H_c values. PBS with lower and higher NaCl concentrations was used for some RBC suspensions in which the osmolality was adjusted to values between 200 and 600 mOsmol kg^{-1} .

RBCs preloaded with AA were prepared as follows: A suspension of RBCs ($H_c \sim 0.50$) in PBS/glucose (5 mM) was incubated with up to 5 mM DHAA at 37 °C for 1 h. During this time all DHAA was reduced to AA or spontaneously converted to extracellular diketogulonic acid (DKG). The RBCs were washed twice with 3 vol of PBS/glucose (5 mM) and then centrifuged (3000g, 5 min, 4 °C). Control ^{13}C NMR spectra of such loaded cells, resuspended in PBS, showed that only intracellular $[1-^{13}\text{C}]\text{AA}$ was present immediately after the preparation.

“Oxidatively prestressed” RBCs were also used. These were prepared by suspending RBCs in PBS/glucose (5 mM) and incubating them with 10–15 mM ferricyanide at 37 °C for 3–4 h. The treated cells were then washed twice with PBS/glucose (5 mM) at 4 °C and centrifuged (3000g, 5 min, 4 °C), and the supernatant was removed. The RBCs were used within minutes of preparation.

H_c values of the RBC suspensions were determined using a hematocrit microcentrifuge (Clements, North Ryde, NSW, Australia). Hemoglobin concentrations and erythrocyte and leukocyte counts were determined electronically using a Sysmex microcell counter (CL-130) and autodilutor (AD-241; Toa Medical Electronics Co., Ltd., Kobe, Japan).

Chemicals. If not otherwise indicated, the chemicals were obtained from Sigma Chemical Co. (St. Louis, MO).

A solution of dimethyl methylphosphonate (DMMP; Fluka AG, Buchs, Germany), hypophosphite (HP; Aldrich, Milwaukee, WI) and methylphosphonate (MeP; Aldrich) in water was prepared for control measurements of pH, volume, and membrane potential of the RBC with various AA/DHAA concentrations (20) (results not shown). The pH was adjusted to ~7.1 with NaOH. When added to suspensions of RBCs, the solution was diluted in phosphate-buffered saline so that the osmolality was ~290 mOsmol kg^{-1} .

The $[1-^{13}\text{C}]$ - and $[2-^{13}\text{C}]\text{AA}$ were synthesized according to Drew et al. (21) by Biochemicals Inc. (South Bend, IN). Fresh 100 mM solutions of ^{13}C -labeled AA in water were usually prepared immediately before use and were never stored for longer than 7 days (at 4 °C). $[1-^{13}\text{C}]$ - and $[2-^{13}\text{C}]\text{-DHAA}$ were produced by oxidation of the respective AA in a solution of ethanol with oxygen gas using an activated charcoal catalyst (22). DHAA was prepared on the day of use, as it is well-known that it is unstable in aqueous solutions (17). Solutions of DHAA were not used after 24 h.

NMR Procedures. ^{13}C , ^{19}F , and ^{31}P NMR spectra were acquired on a Bruker AMX400 wide-bore spectrometer with operating frequencies for ^{13}C , ^{19}F , and ^{31}P of 100.31, 376.43, and 161.98 MHz, respectively. Some ^{13}C NMR spectra were obtained on a Bruker AMX600 spectrometer with an operating frequency of 150.92 MHz.

In the time course experiments, the ^{13}C -labeled compounds were added to thermally equilibrated RBC suspensions (37 °C) immediately before the start of the measurement ($t = 0$ min). Inverse gated decoupling was used to minimize sample heating and enhancements in resonance intensities of ^{13}C nuclei due to the nuclear Overhauser effect.

(D,L)- $[3-^{13}\text{C}]\text{serine}$ (3 mM) was added to some samples in the ^{13}C NMR time course experiments, when an internal standard was required. Concentrations were determined after an automatic baseline correction from the integrals of the ^{13}C NMR signals. In cases of overlapping signals, the integration of the signals was carried out after deconvolution using the Bruker (*uxnmr*) deconvolution software. Typically, between 64 and 512 transients (depending on the concentrations of the ^{13}C -labeled compounds and the H_c of the RBC suspension) were averaged into 16K data points, with a spectral width of 12 000 Hz. A relaxation delay of $5T_1$ was routinely used; however, relaxation delays of only 2 s were applied for experiments in which reactions proceeded too fast to be monitored in the fully relaxed mode or in which low ^{13}C -AA or ^{13}C -DHAA concentrations were used. For quantification of the rapid pulsing time course experiments, a calibration was necessary. Calibration was performed on two identical samples: for both, the ^{13}C NMR spectra were acquired over the same time period, but one sample was run with full relaxation, and the other, with rapid pulsing (more transients for the latter). The ratio of the intensity (area) of

a resonance in each spectrum yielded the calibration factor. The T_1 for the $1\text{-}^{13}\text{C}$ NMR signal of the extracellular AA (10.5 s) was used as the basis for relaxation delays in fully relaxed spectra (intertransient delay, $d1 = 50$ s). This T_1 was longer than those of all other used signals, including T_1 for the intracellular $[1\text{-}^{13}\text{C}]\text{AA}$ (4.1 s).

Samples containing cells were not spun to avoid cell packing in the NMR tube. The probe thermostat setting was adjusted in some ^{13}C NMR time courses according to the method of Bubb et al. (23).

Competitive inhibition of glucose transport was studied by comparing the rates of 3-fluoro-3-deoxyglucose exchange across RBC membranes in the presence and absence of AA and DHAA. The exchange rates were determined by ^{19}F NMR magnetization exchange spectroscopy according to Potts and Kuchel (24).

^{31}P NMR time course experiments were used to determine changes in the mean cell volume, the intra- and extracellular pH, and the membrane potential ($\Delta\Psi$) of the RBC according to Kirk and Kuchel (19, 25, 26) and Kirk et al. (27). The cell suspensions in PBS/glucose (5 mM) were incubated with DMMP (5 mM), HP (5 mM), and MeP (5 mM) at 37 °C for 10 min. ^{31}P NMR time course experiments were performed over a period of ~ 10 h on a suspension in PBS with only glucose or with AA (0.8, 2, and 8 mM) or DHAA (0.8, 2, and 6 mM). The osmolality of the solution was adjusted to 290 mOsmol kg^{-1} , and the H_c of the suspension was 0.7.

Numerical Procedures. Data were processed using CA-Cricket Graph III, version 1.0 (Computer Associates Inc., Malvern, PA) on a Macintosh PowerPC. Reaction rates were determined by regression of a low-degree (1–3) polynomial or the appropriate exponential expression onto the data. Nonlinear regressions (such as the Michaelis–Menten equation) were carried out using the program Origin 3.54 (Microcal Software, Inc., Northampton, MA) on an IBM 486 computer.

RESULTS

RBC Integrity. To avoid artifactual results in studies of DHAA reduction, it was important to maintain the integrity of RBCs incubated for several hours. DHAA could be reduced by the release from lysing cells of several redox metabolites including reduced glutathione (GSH), ergothioneine, and NAD(P)H (e.g., refs 30 and 31). At high concentrations (> 1 mM) of DHAA, lysis of human RBCs (28) and other cells (29) is known to occur. Thus, the extent of hemolysis was monitored by recording cell counts and hematocrits, before and after the time courses. Also, ^{31}P NMR chemical shift differences of the intra- and extracellular populations of added DMMP were used, in a manner described previously (25, 32), to monitor changes in the cell volume and the extent of cell lysis.

Table 1 shows that no major changes in the number of cells occurred with DHAA concentrations up to 2 mM, and AA concentrations up to 10 mM, within the first 2 h of a time course; the extent of lysis was not different from controls ($\sim 3\%$).

The measurement of pH during the incubation of the RBC suspensions showed that the pH in control experiments and in the presence of AA or DHAA remained constant for 1–2 h and decreased afterward by 0.2 unit within 6 h. The

Table 1: The Effect of Different Incubation Media on the Time Dependence of RBC Lysis^a

incubation time	suspension medium and extent of RBC lysis		
	PBS/5 mM glucose	PBS/5 mM glucose + 0.1/2.0/10.0 mM AA	PBS/5 mM glucose + 0.1/2.0/10.0 mM DHAA
1 h	<1%	<1%/<1%/<1%	<1%/1%/1%
2 h	1%	2%/3%/3%	3%/3%/4%
8 h	5%	4%/5%/5%	5%/7%/10%

^a Hematocrits were adjusted to 0.6 before the start of the time courses. The extent of lysis was determined from the peak separation between the intra- and extracellular DMMP signals and the intensities of these signals (see Results).

membrane potential in the presence of AA or DHAA increased more than it did in control experiments, where it increased from -11 to -7 mV within 8 h. This increase was dependent on the concentration of AA and DHAA (e.g., from -10 to -6 mV for 0.5 mM AA and from -10 to -4 for 2 mM AA). A complete analysis of the pH and membrane potential data will be published elsewhere.

"Split-Peak" Phenomenon of ^{13}C -AA. The ^{13}C NMR signals of $[1\text{-}^{13}\text{C}]$ - (see Figure 1) and $[2\text{-}^{13}\text{C}]\text{AA}$ in an RBC suspension in PBS were both split into partially resolved peaks, with separations of 11–15 and 6–10 Hz, respectively (operating frequency, 100.3 MHz). The extent of splitting depended on the osmolality of the suspension medium (which was varied between 250 and 350 mOsmol kg^{-1}) and the concentration of AA. An increase in the osmolality to 500 mOsmol kg^{-1} resulted in a peak separation of 35 Hz for $[1\text{-}^{13}\text{C}]\text{AA}$. At the higher spectrometer frequency of 150.9 MHz the splitting was 17–23 Hz for $[1\text{-}^{13}\text{C}]\text{AA}$ and 10–15 Hz for $[2\text{-}^{13}\text{C}]\text{AA}$. The basis of this phenomenon is the reduced average extent of hydrogen bonding between solvent water and the $[1\text{-}^{13}\text{C}]\text{AA}$ carbonyl group and the $[2\text{-}^{13}\text{C}]\text{AA}$ hydroxyl group, respectively, inside the cells (33). Thus, the splitting of the peaks formed the basis of experiments that enabled the facile identification of relative amounts of intra- and extracellular ascorbate in a cell suspension, without the requirement to isolate and extract the cells. Due to the much larger split-peak effect for $[1\text{-}^{13}\text{C}]\text{AA}$, compared with $[2\text{-}^{13}\text{C}]\text{AA}$, this compound was preferred for use in investigations of AA transport.

Transport of ^{13}C -AA. Because the transport of AA into RBCs is very slow, it was possible to monitor the process by acquiring sequential ^{13}C NMR spectra (Figure 1); the signal from the extracellular AA decreased, whereas the signal for the intracellular AA increased. This proceeded until a steady-state distribution of AA was established between the intra- and extracellular compartments.

Time courses of AA uptake were recorded for a range of initial AA concentrations (0.5–15 mM) (Figure 1A). They were all fitted well by a single-exponential function, all with approximately the same rate constant. [It might have been anticipated that the transport process would be saturable and, hence, the concentration dependence of the rate would be describable by a Michaelis–Menten function; this was not the case, and so implied a K_M that was substantially greater than 15 mM or that the process could involve only passive diffusion (see Discussion for further comments).] Hence, the simplest first-order two-site exchange process that could be used to describe the data was employed; it has the

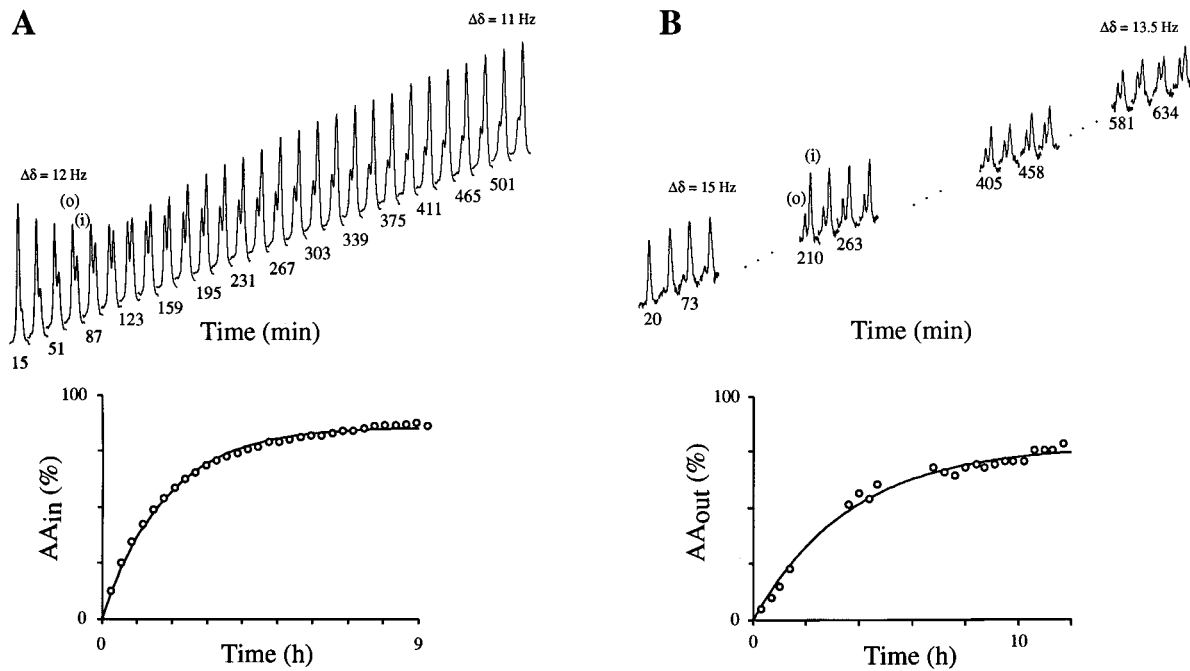


FIGURE 1: ¹³C NMR spectra of [1-¹³C]AA acquired in a time course after (A) AA had been added to RBCs suspended in PBS/glucose (5 mM) and (B) RBCs were loaded with [1-¹³C]AA and resuspended in PBS/glucose (5 mM). The amounts of [1-¹³C]AA were calibrated with respect to internal [3-¹³C]serine (4 mM). The chemical shift range in the plot was 178–178.5 ppm. NMR acquisition parameters: intertransient delay, 50 s; number of transients, 16 (A) and 32 (B). Numbers under the spectra refer to the time (min) at which half of the transients were acquired for each spectrum. The pH was 6.9, and T = 37 °C; (o) and (i) refer to the extra- and intracellular [1-¹³C]AA, respectively. Plots of the relative amounts (%) of [1-¹³C]AA in the intracellular (A) and extracellular (B) compartments, respectively, as a function of time are shown below the respective spectra. The total amount of [1-¹³C]AA in the RBC suspension is denoted as 100%. The relative amounts of [1-¹³C]AA were determined from spectral integration after baseline correction and deconvolution of the overlapping peaks. Nonlinear least-squares regression of eqs 1 and 2 onto the data yielded the rate constants for the influx and efflux, respectively. For influx (A) the total amount of AA was 15 mmol per liter of sample volume, and H_c = 0.81. The fitted parameter values were $k_1 = (1.14 \pm 0.03) \times 10^{-4} \text{ s}^{-1}$ and $k_{-1} = (0.27 \pm 0.04) \times 10^{-4} \text{ s}^{-1}$; these two values were used in conjunction with eqs 3 and 4 to calculate $P_1 = (1.3 \pm 0.1) \times 10^{-6} \text{ cm s}^{-1}$ and $P_{-1} = (1.2 \pm 0.1) \times 10^{-6} \text{ cm s}^{-1}$, respectively. For efflux (B) the total amount of AA was 3.5 mmol per liter sample volume and H_c = 0.60; the fitted parameter values were $k_1 = (0.5 \pm 0.05) \times 10^{-4} \text{ s}^{-1}$ and $k_{-1} = (0.28 \pm 0.04) \times 10^{-4} \text{ s}^{-1}$; the respective calculated values of the permeabilities were $P_1 = (1.2 \pm 0.15) \times 10^{-6} \text{ cm s}^{-1}$ and $P_{-1} = (1.2 \pm 0.1) \times 10^{-6} \text{ cm s}^{-1}$.

following mathematical form (e.g., ref 34):

$$AA_{\text{ex}} = AA_0 k_1 (k_1 + k_{-1})^{-1} (k_{-1} (k_1)^{-1} + \exp(-(k_1 + k_{-1})t)) \quad (1)$$

and

$$AA_{\text{in}} = AA_0 k_1 (k_1 + k_{-1})^{-1} (1 - \exp(-(k_1 + k_{-1})t)) \quad (2)$$

where k_1 and k_{-1} are the apparent first-order rate constants for the influx and efflux, respectively. AA_0 , AA_{in} , and AA_{ex} denote the total amount (mol) of AA and the amounts of AA in the intra- and extracellular compartments at a given time, respectively.

Nonlinear least-squares regression of eqs 1 and 2 onto a graph of the NMR peak intensities, as a function of time, yielded estimates of the apparent rate constants and their associated standard deviations (Figure 1). These apparent rate constant values were used to obtain estimates of the membrane permeability coefficients for influx (P_1) and efflux (P_{-1}) (Table 2), using the formulas

$$P_1 = \text{MCV}(1 - H_c)k_1 A^{-1} H_c^{-1} \quad (3)$$

and

$$P_{-1} = \alpha \text{MCV} k_{-1} A^{-1} \quad (4)$$

where α is the fraction of the intracellular volume that is freely accessible to solutes, MCV is the mean cell volume (84–90 fL, depending on the donor), and A is the mean cell surface area (143 μm^2 ; 35). This form of normalization is important because, in contrast to the first-order rate constants, the apparent P_1 and P_{-1} values are independent of the hematocrit (H_c) (e.g., ref 24).

Alternatively, the analysis of the time course data for AA influx was also performed using the initial uptake rates for AA. The values for the initial velocity were comparable to $k_1[AA]_0$, where $[AA]_0$ is the total concentration of AA in the cell suspension (Figure 1).

DMMP was used with ³¹P NMR to determine the intracellular volume of the RBC that is freely accessible to solutes (32). Hence, these data were used to determine the concentration of AA inside and outside the RBC. The final concentration of AA inside the RBC, after a steady-state (quasi-equilibrium) had been established, was typically 1.5–2.5 times higher than the concentration outside the RBC.

P_1 and P_{-1} values were determined from blood obtained from three different donors. There was no concentration dependence of P_1 and P_{-1} with $[AA]$ in the range 0.5–15 mM, and there were no significant differences in P_1 and P_{-1} values between the samples.

Effects of Inhibitors on AA Transport. Several different inhibitors of transport systems in RBCs and of glycolysis

Table 2: Incubation and Inhibitor Conditions Affecting the Membrane Permeability Coefficient for Influx (P_1) and Efflux (P_{-1}) of AA in RBCs

treatment ^a	<i>n</i> ^a	$P_1 \pm \text{SD}^a$ (10^{-9} cm s ⁻¹)	$P_{-1} \pm \text{SD}^a$ (10^{-9} cm s ⁻¹)
none	10	1.3 \pm 0.3	1.4 \pm 0.3
RBCs loaded with [1- ¹³ C]AA (transport inside-out) ^b	4	1.1 \pm 0.2	1.2 \pm 0.3
NaF (0.5 mM) + iodoacetate (0.5 mM) ^c	3	1.2 \pm 0.4	1.3 \pm 0.4
replacement of glucose by 2-deoxyglucose in PBS ^c	3	1.3 \pm 0.3	1.3 \pm 0.3
no glucose ^c	2	1.2 \pm 0.2	1.3 \pm 0.3
replacement of 5 mM glucose by 1 mM glucose	2	1.3 \pm 0.2	1.1 \pm 0.2
replacement of 5 mM glucose by 150 mM glucose	2	1.2 \pm 0.1	1.3 \pm 0.2
4,4'-dinitrostilbene-2,2'-disulfonate (100 μ M) ^d	2	1.3 \pm 0.1	1.3 \pm 0.1
<i>p</i> -CMPS (100 μ M) ^d	2	0.8 \pm 0.1	0.7 \pm 0.2
cytochalasin B (50 μ M) ^d	3	0.2 \pm 0.05	0.2 \pm 0.05
phloretin (100 μ M) ^d	4	0.2 \pm 0.05	0.2 \pm 0.05
1-chloro-2,4-dinitrobenzene (100 μ M)	2	1.3 \pm 0.1	1.1 \pm 0.2
RBCs loaded with [1- ¹³ C]AA and afterwards incubated with phloretin (80 μ M) (transport inside-out) ^b	2	0.2 \pm 0.1	0.2 \pm 0.1

^a The concentration of AA was 0.5–15 mM, and the H_c was 0.5–0.7. *n*, number of repetitions. SD, standard deviation. ^b [1-¹³C]AA was added to a suspension of RBCs in PBS/5 mM glucose. ^c RBCs were preincubated for 30 min before [1-¹³C]AA was added. ^d Short preincubation with the respective compound at 37 °C for 10 min, before the ¹³C NMR measurement was started.

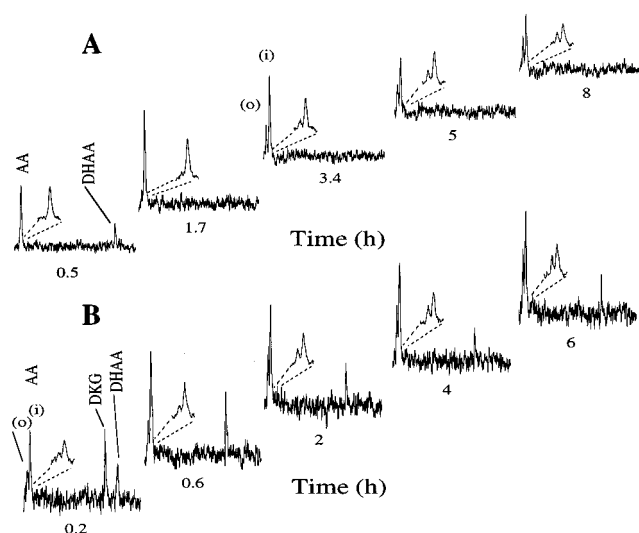


FIGURE 2: Selected ¹³C NMR time courses of a suspension of RBCs in PBS/glucose (5 mM) to which [1-¹³C]DHAA at a concentration of (A) 1.5 mM or (B) 4.4 mM was added at $t = 0$ h. The H_c was 0.6 for both experiments. NMR acquisition parameters: intertransient delay, 15 s (A) and 45 s (B); number of transients, 192 (A) and 32 (B). The chemical shift range in the plots was 172.0–178.5 ppm. Baseline correction was used, and the numbers under each spectrum refer to the time (h) at which half of the transients were acquired for each spectrum; (o) and (i) refer to the extra- and intracellular [1-¹³C]AA, respectively.

had effects on the transport of [1-¹³C]AA into RBCs; these results are reported in Table 2.

AA uptake as monitored by ¹³C NMR was inhibited only by the specific inhibitors of glucose transporters (phloretin and cytochalasin B) and by *p*-chloromercuriphenylsulfonate (*p*-CMPS). No inhibition was effected by glucose concentrations up to 150 mM. The very fast transmembrane exchange of 3-fluoro-3-deoxyglucose (5 mM), monitored by ¹⁹F NMR magnetization transfer (36), was not affected by the addition of either AA or DHAA (up to 20 mM each). The permeability for the fluoroglucose at 5 mM was found to be $4.1 \pm 0.4 \times 10^{-5}$ cm s⁻¹ for the α anomer and $3.6 \pm 0.4 \times 10^{-5}$ cm s⁻¹ for the β anomer in the presence or absence of either AA or DHAA up to 15 mM.

The measured membrane permeabilities for efflux, in the presence and absence of inhibitors, were seen to be equal to those obtained from the experiments on influx of AA (last column, Table 2).

Transport and Reduction of DHAA. ¹³C NMR spectra were acquired from RBC suspensions to which [1-¹³C]- or [2-¹³C]DHAA (total concentrations of 0.5–10 mM) was added; typical NMR time courses from the incubation of a suspension containing [1-¹³C]DHAA are shown in Figure 2. Because of the high rate of the reaction, it was not possible to monitor DHAA reduction by acquiring fully relaxed spectra, if the concentration of DHAA was less than 2 mM. Thus, a rapid pulsing method and calibration factors were used to quantify the reduction rates (see Materials and Methods). For the higher concentrations of DHAA the time courses of increase in AA signal were almost linear over tens of minutes (Figure 2), thus enabling more precise measurement of the initial velocity of the reaction.

Since DHAA is very unstable at physiological pH (17, 37), other peaks became *relatively* large in the NMR spectra when either lower H_c values or higher DHAA concentrations were used (Figure 2B). The additional NMR peaks were shown to be due to degradation products of DHAA, mainly diketogulonic acid (DKG), that further spontaneously degraded to oxalic acid and CO₂ (38). The reduction rate of DHAA was much faster than the transport rate of AA into the cells, as is already known (13–16); and 90–60% of the initial DHAA was reduced using initial concentrations of 3–10 mM.

In experiments with lower DHAA concentrations (<2 mM), almost all of the AA which was formed from it was detected *inside* the RBC, as evidenced by the location of the ¹³C NMR split peak. Importantly, from the perspective of the mechanism of DHAA uptake and reduction, this intracellular AA subsequently effluxed from the cells with the same rate as for RBCs preloaded with AA (vide supra). With an increase of the DHAA concentration (3–9 mM), the extracellular AA formed from DHAA increased in comparison with the intracellular AA (Figure 2 and Tables 3 and 4). In other words, not all of the AA was formed inside the RBC. A similar outcome

Table 3: Factors Affecting the Rate of DHAA Reduction in a Suspension of RBCs^a

treatment	<i>n</i> ^b	rate of DHAA redn ^c
NaF (0.5 mM) + iodoacetate (0.5 mM)	5	<5% ^d
replacement of glucose by 2-deoxyglucose in PBS	5	<5% ^d
no glucose	3	<5% ^d
replacement of 5 mM glucose by 1 mM glucose	2	100%
replacement of 5 mM glucose by 150 mM glucose	2	100%
with ferricyanide prestressed RBCs ^e	6	35–60%
4,4'-dinitrostilbene-2,2'-disulfonate (100 μM) ^f	2	100%
<i>p</i> -CMPS (100 μM) ^f	3	30–40%
cytochalasin B (50 μM) ^f	4	100%
phloretin (100 μM) ^f	4	100%
1-chloro-2,4-dinitrobenzene (100 μM) ^f	5	50–80%

^a The rate of DHAA reduction was calculated from the rate of AA formation. DHAA concentrations varied between 2 and 6 mM. The *H_c* was 0.55–0.65, and the RBCs were incubated in the NMR spectrometer with [1-¹³C]- or [2-¹³C]DHAA for 2–7 h at 37 °C. ^b *n*, number of repetitions. ^c The rate of DHAA reduction was compared with a control experiment in which the reduction of DHAA was monitored in a suspension of RBCs in PBS/glucose (5 mM). ^d RBC were preincubated for 30 min before ¹³C-labeled DHAA was added. An initial reduction of 0.2–0.3 mmol (L of RBCs)^{−1} DHAA occurred. The remaining DHAA was degraded almost completely to DKG. ^e RBCs (*H_c* ~ 0.15) were incubated with ferricyanide (10–15 mM) as in Materials and Methods. ^f Short preincubation with the respective compound at 37 °C for 10 min, before the ¹³C NMR measurements were begun.

was observed at lower *H_c* values (~0.30).

The concentration dependence of the initial rate of reduction of DHAA by RBC followed Michaelis–Menten kinetics (Figure 3).

Potential Effectors of DHAA Reduction. DNDS, an inhibitor of the RBC anion transporter (band 3), had no influence on the rate of DHAA reduction (Table 3). Also, the inhibitors of the glucose transporter, phloretin and cytochalasin B, had no influence on the rate of reduction of DHAA or on the distribution of intra- and extracellular AA found immediately after the reduction was complete. However, the consecutive efflux of the reduced intracellular AA was inhibited to the same extent as was the efflux in the experiments with cells preloaded with AA (Table 3), and there was no evidence of (competitive) inhibition by high concentrations of glucose.

Incubation with inhibitors of glycolysis or incubation with no glucose or 2-deoxyglucose strongly inhibited the reduction of DHAA. Apart from a small amount of initially reduced DHAA [<0.3 mmol (L of RBCs)^{−1}], no further formation of AA was observed, and the DHAA signal intensity declined due to its degradation to DKG. The rate of DHAA degradation to DKG was similar to that monitored in a PBS solution without RBCs (first-order kinetics, half-life ~50 min). In these experiments no splitting of the DHAA signal or of the resulting DKG signal into peaks representing the intra- and extracellular populations was seen, and both signals were much more intense and stable than in metabolically active RBCs.

Oxidatively prestressing the RBCs with ferricyanide (see Materials and Methods) led to the inhibition of DHAA reduction (Table 3). The reaction rates varied between 1.3 (for 0.8 mM DHAA) and 2.8 mmol (L of RBCs)^{−1} h^{−1} (for 4 mM DHAA).

Incubation with 1-chloro-2,4-dinitrobenzene (CDNB) and *p*-CMPS also yielded a measurable but incomplete

inhibition of DHAA reduction (Table 3). [CDNB is known to decrease GSH concentration by conjugation to the sulfhydryl group in a reaction catalyzed by glutathione-*S*-transferase (39), and *p*-CMPS is known not to permeate the cell membrane but affects the activity of some membrane transporters that have mechanistically important sulfhydryl groups (40).]

In another series of experiments, the reduction of [1-¹³C]-DHAA was monitored in a suspension of RBCs preloaded with unlabeled AA (0.1–0.4 mM; see Table 4). In addition to the expected slightly faster reduction of DHAA and a reduced amount of degradation products (DKG), these RBCs yielded a much lower ratio of intra- to extracellular [1-¹³C]-AA after attainment of a steady state. Less [1-¹³C]AA was found inside the RBC than observed without preloading. This result was independent of the presence of inhibitors of glucose transport. Thus, the results indicated that the intracellular AA reduced extracellular DHAA. To investigate this further (see Figure 4), RBCs were preloaded with [2-¹³C]AA (1 mM) and then resuspended in PBS containing [1-¹³C]DHAA (total concentration after resuspension, 4.1 mM). The (exclusively) intracellular [2-¹³C]-AA was first oxidized by the extracellular [1-¹³C]DHAA to [2-¹³C]DHAA and then rereduced inside the cells to [2-¹³C]AA. The reduction of the added [1-¹³C]DHAA again was faster than without preloading, and the ratio of intracellular to extracellular [1-¹³C]AA after the reduction was complete was much lower than without the intracellular [2-¹³C]AA.

[1-¹³C]DHAA Split-Peak Phenomenon. Using ¹³C NMR, it was not possible to measure the permeation of DHAA into RBCs separately from its reduction, since no split peak was evident in the spectra. This was surmised to be due to either the rapid reduction of DHAA inside the cells or the absence of a split-peak phenomenon. In addition, no peak splitting was evident for DHAA with metabolically inactive RBCs (as used for experiments reported in Table 3).

In view of the above observations, the dependence of the chemical shifts of [1-¹³C]AA, [1-¹³C]DHAA, and [1-¹³C]-DKG on the concentration of hemoglobin added to the respective solutions was determined (Figure 5). A very similar dependence of the chemical shift on hemoglobin concentration was found for both of [1-¹³C]AA and [1-¹³C]-DHAA. The extent of peak splitting was such that if a significant amount of DHAA were present intracellularly, it would give a peak whose chemical shift would be distinctly different from DHAA outside the cells. Therefore, the absence of peak splitting in the ¹³C NMR spectra implied that DHAA was in only one compartment.

The chemical shift of DKG was not strongly dependent on the hemoglobin concentration (Figure 5). Thus, no measurable peak splitting would be expected for DKG distributed inside and outside RBCs. Furthermore, DKG did not permeate the RBC as evidenced by the fact that RBCs incubated with ~10 mM [1-¹³C]DKG for 1 h and then washed and resuspended in PBS yielded no ¹³C NMR signal.

The results for the chemical shift of the [1-¹³C]AA peak in Figure 5 are in agreement with the *in vitro* experiments. The hemoglobin concentration in the RBCs used for the experiments on AA transport was typically 29–33 g/dL, which corresponds to a shift in the chemical shift of 11–13

Table 4: Comparison of Distribution and Production of Derivatives of [1-¹³C]DHAA in an RBC Suspension after the First Data Point ($t = 20$ min) and after 3 h^a

treatment	t = 20 min				t = 3 h				AA _{in} /AA _{ex}	rate of DHAA redn (mmol (L of RBCs) ⁻¹ h ⁻¹)
	DHAA	DKG	AA _{in}	AA _{ex}	DHAA	DKG	AA _{in}	AA _{ex}		
none	38%	11%	43%	5%	0%	6%	64%	23%	2.7	7.2
[DHAA] = 6 mM	46%	17%	23%	9%	0%	16%	46%	22%	2.1	9.2
phloretin (100 μM) ^b	37%	10%	46%	4%	0%	7%	77%	8%	9.6	7.3
NaF + iodoacetate (each 0.5 mM) ^b	71%	21%	0%	5%	11%	35%	0%	5%		<0.5
with AA (0.2 mM) preloaded RBCs ^c	29%	8%	36%	22%	0%	4%	59%	33%	1.8	8.1

^a The experimental conditions were the same as listed for the experiments below: same blood donor, $H_c = 0.62$, and $[[1-^{13}\text{C}]\text{DHAA}] = 3$ mM (unless otherwise indicated). The ratio of intra- to extracellular volume in the RBC suspension was determined to be $V_{in}/V_{ex} = 1$. The steady-state distribution of $\text{AA}_{in}/\text{AA}_{ex}$ was ~ 1.9 . The initially added concentration of DHAA was set to 100%. ^b RBCs were preincubated with the listed compounds for 15 min before ¹³C-labeled DHAA was added. ^c RBCs were preloaded with unlabeled AA and washed twice in PBS before ¹³C-labeled DHAA was added.

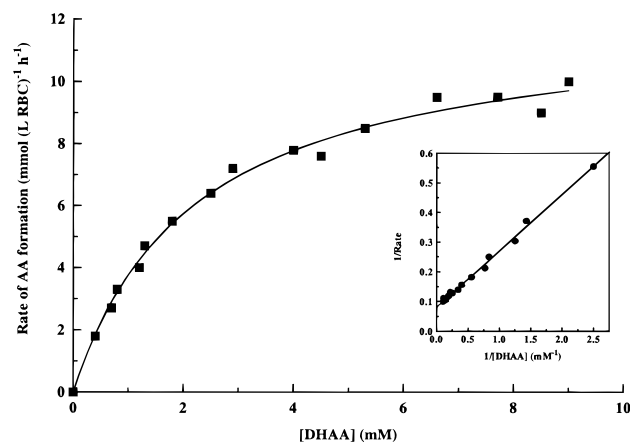


FIGURE 3: Concentration dependence of the rate of DHAA reduction in a suspension of RBCs in PBS/glucose (5 mM). The H_c was between 0.64 and 0.71. The initial rates were determined from the rates of AA formation in the reaction (total concentration of AA). The DHAA concentrations refer to the initial DHAA concentrations (total), independent of how much DHAA was reduced to AA or degraded to DKG. A nonlinear least-squares regression of the Michaelis–Menten equation onto the data yielded the value of the maximal velocity ($V_{max} = 12.1 \pm 0.3$ mmol (L of RBCs)⁻¹ h⁻¹) and the Michaelis constant ($K_M = 2.2 \pm 0.2$ mM). The corresponding Lineweaver–Burk plot is depicted in the inset, to visually reinforce the Michaelis–Menten nature of the kinetic data.

Hz. The separation between the extra- and intracellular peaks of [1-¹³C]AA in an RBC suspension was 11–15 Hz.

Extracellular Oxidative Stress and AA Transmembrane Flux. RBCs loaded with 1.5 mM [1-¹³C]AA were suspended in PBS/glucose containing 10–20 mM ferricyanide (see Materials and Methods). [Human RBCs are able to reduce extracellular ferricyanide at rates up to ~ 20 mmol (L of RBCs)⁻¹ h⁻¹ in the presence of 1.5 mM intracellular AA (4).] All the extracellular ferricyanide would have been reduced within 1.5–2 h in an RBC suspension with an H_c of 0.5–0.7; this would correspond to the first two or three spectra in an NMR time course of efflux of [1-¹³C]AA (Figure 1B). However, the intracellular AA was oxidized to DHAA, and then the DHAA was (>90%) reduced back to AA after completion of the reduction of the extracellular ferricyanide. Furthermore, almost all of the AA remained inside the RBC after all of the ferricyanide had been reduced, and its efflux proceeded with the same rate as was measured for the resting preloaded RBCs (vide supra).

The use of an RBC suspension with exclusively extracellular [1-¹³C]AA at the time of ferricyanide addition yielded

a distribution of extra- and intracellular [1-¹³C]AA, after the DHAA recycling, that was close to the expected steady-state distribution, with slightly more AA inside the cells.

No significant differences in the rate of ferricyanide reduction and DHAA recycling were found between these different experiments.

DISCUSSION

Split-Peak Phenomenon with AA and DHAA. The finding of the ¹³C NMR split peaks with [1-¹³C]AA in RBC suspensions enabled a very simple means of following the transport of AA into and out of the cells (Figure 1). It also afforded a simple means of determining the site of the associated oxidation and reduction reactions of both compounds.

AA Transport. Conventional methods used to study AA transport and metabolism that entail adding radiolabeled compounds to RBC suspensions require the separation of the various components of the reactions to obtain quantitative kinetic data. The former results indicate that AA is transported into the RBC via the glucose transporter (8), or alternatively, it is transported via a similar transporter, with high specificity for AA, but which is also inhibited by phloretin and cytochalasin B. Evidence for the second mechanism, or for a higher affinity by the glucose transporter for AA than glucose, is the finding that no competitive inhibition was observed between glucose transport and AA transport. Simple diffusion, as previously described (7, 14), does not significantly contribute to the transport of AA into the RBC, since the inhibition of transport by inhibitors of the glucose transporter was almost complete (Table 2). The inhibition of the transport by *p*-CMPS provided evidence for the involvement of sulfhydryl groups of membrane proteins (40) in AA transport.

DHAA Transport. In contrast to results obtained by others (8, 11), DHAA transport was seen *not* to be affected by inhibitors of the glucose transporter, and there was no indication of inhibition by glucose itself. In contrast, Bianchi and Rose (15) reported that 20 mM glucose is the maximally inhibitory concentration for DHAA transport, and yet they suggested the existence of an additional, glucose-independent system of DHAA transport in RBCs. Their results indicated that this transport system is that which is relevant at physiological glucose concentrations (~ 5 mM). Our findings support the existence of such a glucose-independent DHAA transporter and suggest that this system is also the *dominant* transporter at the high DHAA concentrations used in the present study.

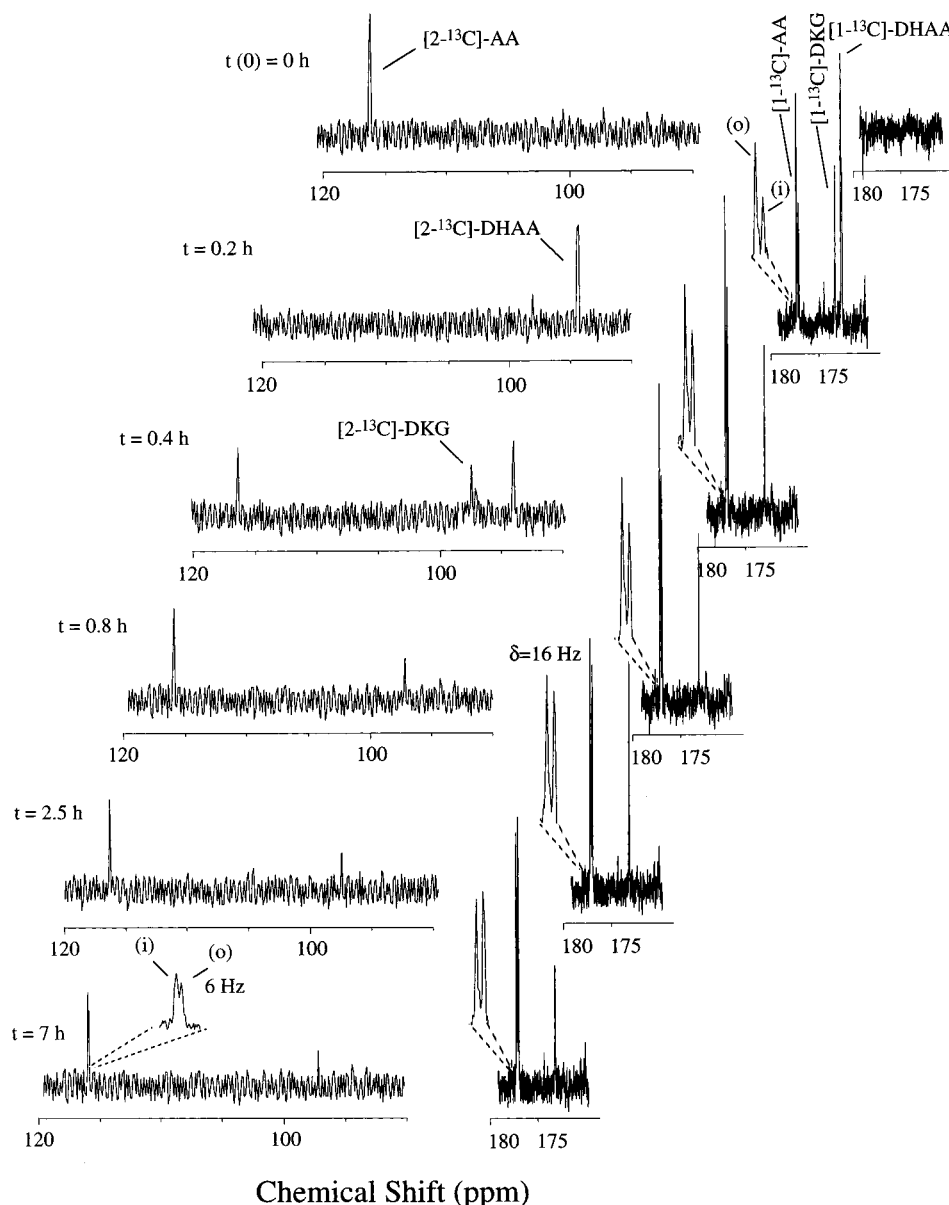


FIGURE 4: RBCs were loaded with 1.1 mM $[2\text{-}^{13}\text{C}]\text{AA}$ [first spectrum at $t(0) = 0$ h]. Afterwards, $[1\text{-}^{13}\text{C}]\text{DHAA}$ (total concentration, 4.1 mM; $H_c = 0.6$) was added to the suspension of the loaded RBCs and a time course was recorded (from the second spectrum at $t = 0.2$ h to the last spectrum at $t = 7$ h). The spectra were acquired in the rapid pulsing mode. For quantification of these spectra, a calibration factor was applied; (o) and (i) refer to the extra- and intracellular populations of the respective compounds. NMR acquisition parameters: intertransient delay, 2 s; number of transients, 448.

Reduction of DHAA Added to the Outside of RBCs. The transport of DHAA appeared to be coupled with its reduction to AA (Table 3). The *transported* DHAA was always converted to intracellular AA, and no evidence of free intracellular DHAA was found. The absence of intracellular DHAA, as evidenced by the absence of the expected splitting of the signals for its intra- and extracellular populations (see Figure 4), suggested that the DHAA was reduced *in the process of its transport* or, alternatively, that immediate reduction occurred after entry into the cell. Evidence for the first proposal lay not only in the fact that the reduction of DHAA was dependent on the metabolic activity of the RBC (Tables 3 and 4) but also that DHAA was not transported into metabolically inactive cells. The latter was shown by the absence of the otherwise expected splitting of the $[1\text{-}^{13}\text{C}]\text{DHAA}$ peak due to the appearance of an intracellular population, in these experiments.

The rates of DHAA reduction represent the outcome of a complex reaction scheme, consisting of several processes including the transport of DHAA, the transmembrane transfer of reducing equivalents, the direct reduction of DHAA, and most importantly the degradation of DHAA to DKG. Notwithstanding the complexity, a Michaelis–Menten plot of the velocity of this *overall* reaction (Figure 3) provided a good “summary” of the data with a K_M of 2.2 ± 0.2 mM and a V_{\max} of 12.1 ± 0.3 mmol (L of RBCs) $^{-1}$ h $^{-1}$. These numbers provide information relevant to a quantitative overview of the rate of ascorbate metabolism in the whole body.

Ferricyanide Provided Extracellular “Oxidative Stress”. Experiments with RBCs that had been preloaded with AA and then exposed to extracellular ferricyanide revealed oxidant-induced AA recycling, as proposed by May et al. (6, 8). This involves the transfer of electrons from AA (but

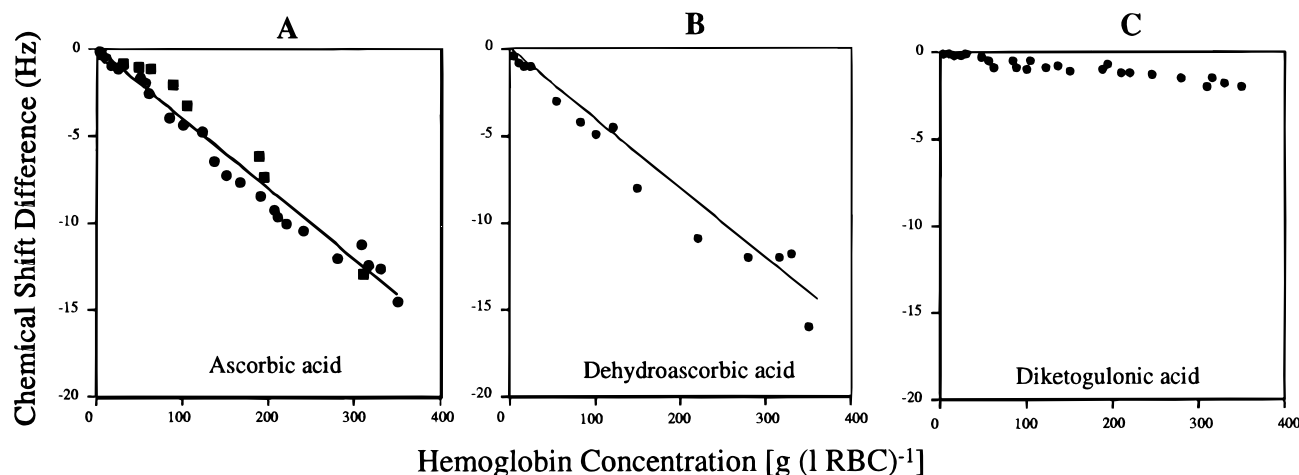


FIGURE 5: Effect of variation of hemoglobin concentration on the chemical shift of $[1\text{-}^{13}\text{C}]\text{AA}$ (A), $[1\text{-}^{13}\text{C}]\text{DHAA}$ (B), and $[1\text{-}^{13}\text{C}]\text{DKG}$ (C). Concentrated hemolysates were prepared by sonicating RBCs. Each sample was diluted with various amounts of PBS. $[1\text{-}^{13}\text{C}]\text{AA}$ and $[1\text{-}^{13}\text{C}]\text{DHAA}$ were added to give a total concentration of 4 mM. Chemical shifts were measured relative to that of $[1\text{-}^{13}\text{C}]\text{glucose}$ (5 mM) in PBS (●) (chemical shift difference here refers to $(\delta_{\text{obs}} - \delta([1\text{-}^{13}\text{C}]\text{glucose})) - (\delta_{\text{obs}} - \delta([1\text{-}^{13}\text{C}]\text{glucose})_{\text{H}_2\text{O}})$) and to $[1\text{-}^{13}\text{C}]\text{AA}$ in PBS/glucose (5 mM) placed in a small spherical bulb, coaxial with the sample tube (■) (chemical shift difference here refers to $(\delta_{\text{obs}} - \delta([1\text{-}^{13}\text{C}]\text{AA in bulb}))$). The chemical shift differences are quoted relative to their values in the absence of hemoglobin. $[1\text{-}^{13}\text{C}]\text{Glucose}$ did not give rise to a significant split peak effect in the present suspensions of RBCs. By measuring chemical shift differences relative to that of $[1\text{-}^{13}\text{C}]\text{glucose}$ and of the chemical shift of a standard placed in a small spherical bulb, the chemical shift effects arising from variations in the magnetic susceptibilities of the samples are eliminated (26).

no transport of AA itself) to extracellular ferricyanide across the membrane, in contrast to the proposal of Orringer and Roer (2) which involves the shuttling of AA across the membrane to directly reduce extracellular ferricyanide.

However, in contrast to the finding of May et al. (8) that extracellular ferricyanide induces a rapid efflux of DHAA from the cells of radioactively labeled AA, we found no evidence of increased DHAA or AA efflux in the presence of ferricyanide. Specifically, exposure of AA-loaded RBCs to extracellular ferricyanide resulted in the complete oxidation of the intracellular AA to DHAA, and after the complete reduction of extracellular ferricyanide, almost all the DHAA (70–100%) was converted back to intracellular AA. This intracellular ^{13}C -AA then effluxed from the RBCs at a rate consistent with the low membrane permeability, determined in experiments on the efflux from resting RBCs (Table 2). Such depletion of intracellular DHAA, as suggested by May et al. (8), appears to be unlikely since intracellular DHAA would be expected to be very rapidly reduced by intracellular GSH and NADPH (31, 41).

The exposure of an RBC suspension to extracellular ferricyanide was repeated with different AA distributions between the intra- and extracellular compartments. Each of the initial distributions yielded the same rate of ferricyanide reduction, indicating that the AA-dependent reduction of ferricyanide and the re-reduction of DHAA are independent of the location of the AA (4, 6). However, since the different pre-experimental AA distributions resulted in different AA distributions after the completion of the ferricyanide reduction reaction, this is evidence of a second mechanism of re-reduction of DHAA, apart from its transport into the cells. This proposal was also supported by the finding that preloading RBCs with AA resulted in different transmembrane steady-state AA distributions, in experiments in which the reduction of ^{13}C -DHAA was monitored. And the steady-state distribution of AA was also affected by the initial ^{13}C -DHAA concentration. The suggested transport-independent mechanism of DHAA reduction is probably the

same as that for the reduction of extracellular ferricyanide (4, 6, 8). A similar system is known for chromaffin granules which lack a transporter for AA (42), but external AA regenerates internal DHAA by electron transfer through the membrane (43, 44). In the case of self-inhibition of the DHAA transport system in RBCs (saturation, or a large extracellular oxidative stress), external DHAA does not become reduced in the course of its transport into the RBC but instead is reduced by a monodehydroascorbyl-free-radical reductase (5, 45), or more likely, by a transmembrane oxidoreductase (9, 46, 47), as suggested for ferricyanide reduction (4, 6, 8).

The results shown in Figure 4 also support an additional AA-transport-independent mechanism of transmembrane electron transfer for high AA concentrations. The exclusively intracellular $[2\text{-}^{13}\text{C}]\text{AA}$ was reduced by extracellular $[1\text{-}^{13}\text{C}]\text{DHAA}$ to $[2\text{-}^{13}\text{C}]\text{DHAA}$. It was not possible to distinguish whether the formed $[2\text{-}^{13}\text{C}]\text{DHAA}$ was inside or outside the RBC. However, the $[2\text{-}^{13}\text{C}]\text{AA}$ formed by re-reduction of $[2\text{-}^{13}\text{C}]\text{DHAA}$ was found almost exclusively inside the RBC after the reduction of the added $[1\text{-}^{13}\text{C}]\text{DHAA}$ was complete. The intracellular $[2\text{-}^{13}\text{C}]\text{AA}$ left the RBC slowly thereafter until transmembrane equilibration was established.

Sources of Electrons in RBCs. The question of the ultimate source of the reducing equivalents for DHAA is relevant to the present results. The transport and recycling of DHAA were strongly dependent on glycolysis in the RBC. Earlier studies on RBC metabolism in the presence of AA and DHAA revealed only minor changes in metabolism, compared with control RBCs; the rate of glycolysis changed insignificantly (ref 4 and results to be published elsewhere). A decrease of 10% occurred in the Rapoport–Luebering shunt flux; an increase of 10% was observed in the pentose phosphate pathway flux, and only a small change occurred in the pyruvate/lactate ratio (4). It was suggested that NADH-dependent processes might be responsible for the operation of the DHAA recycling at low DHAA concentra-

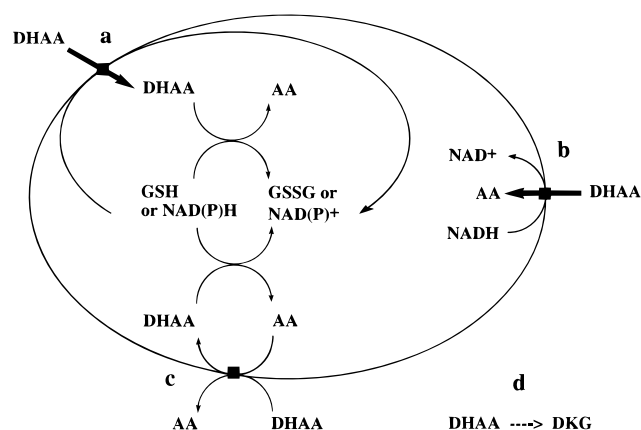


FIGURE 6: Proposed model of vitamin C redox cycling in RBC, based on a model by May et al. (8): (a) DHAA enters the cell via the glucose transporter and becomes reduced to AA, via GSH or NADPH oxidation (at concentrations > 0.4 mM this probably carries the main flux). (b) DHAA enters the RBC via a glucose-transporter-independent system and becomes reduced, most likely in the course of transport via processes related to NADH oxidation (at concentrations < 0.4 mM this probably carries the main flux). (c) A slower competitive process to process b is the transfer of reducing equivalents via a transmembrane oxidoreductase, which depends on oxidation of intracellular AA which by itself becomes re-reduced via GSH oxidation. (d) At high concentrations of DHAA the irreversible degradation of DHAA to DKG and other compounds occurs at a relatively high rate. For a complete description of vitamin C recycling in RBC suspensions, at least the reactions shown here must be considered.

tions (3, 8, 45). However, in experiments in which AA-loaded RBCs were exposed to extracellular ferricyanide, a significant increase in the pentose phosphate pathway flux, and a decrease in the ratio of GSH/oxidized glutathione, was detected. These results suggested that intracellular DHAA, which was formed in the process of electron transfer to extracellular oxidants, was recycled via intracellular GSH [and pentose phosphate pathway (NADPH/GSH)-dependent processes]. Thus, the results suggest the involvement of both NADH and NADPH in the recycling of DHAA. These findings were also supported by the present experiments in which GSH was depleted by alkylation with 1-chloro-2,4-dinitrobenzene (Table 3). Since its inhibitory effect strongly depends on the DHAA concentration and on AA-preloading of the RBCs, there appeared to be processes involved in the DHAA reduction that depended on intracellular GSH.

Model of Redox Reactions and Transport of AA and DHAA in RBC Suspensions. An extension of the model of vitamin C redox cycling in RBCs was based on that proposed by May et al. (8); it is shown in Figure 6. Thus Figure 6 is a summary of our current interpretation of ascorbate transport and redox cycling in human RBCs. In experiments with high DHAA concentrations (> 5 mM) and low hematocrits, cell lysis and degradation of DHAA leads to additional sources of reducing equivalents that reduce DHAA; however, these processes are not anticipated to be physiologically important, so they are not included in the model.

ACKNOWLEDGMENT

Drs. W. A. Bubb, B. E. Chapman and A. Torres are thanked for assistance and discussions with respect to NMR spectroscopy, and Mr. P. J. Mulquoney is thanked for valuable discussions on erythrocyte metabolism. Mr. W. G. Lowe is thanked for expert technical assistance.

REFERENCES

- Englard, S., and Seifter, S. (1986) *Annu. Rev. Nutr.* 6, 365–406.
- Orringer, E. P., and Roer, M. E. (1979) *J. Clin. Invest.* 63, 53–58.
- Schimpfer, W., Neophytou, B., Trobisch, R., Groiss, O., and Goldenberg, H. (1985) *Int. J. Biochem.* 17, 819–823.
- Himmelreich, U., and Kuchel, P. W. (1997) *Eur. J. Biochem.* 246, 638–645.
- Goldenberg, H., Grebing, C., and Löw, H. (1983) *Biochem. Int.* 6, 1–9.
- May, J. M., Qu, Z., and Whitesell, R. R. (1995) *Biochim. Biophys. Acta* 1238, 127–136.
- Hughes, R. E., and Maton, S. C. (1968) *Br. J. Haematol.* 14, 247–253.
- May, J. M., Qu, Z., and Whitesell, R. R. (1995) *Biochemistry* 34, 12721–12728.
- Zamudio, I., Cellino, M., and Canessa-Fischer, M. (1969) *Arch. Biochem. Biophys.* 129, 336–345.
- Basu, S., Som, S., Deb, S., Mukherjee, D., and Chatterjee, I. B. (1979) *Biochem. Biophys. Res. Commun.* 90, 1335–1340.
- Mann, G. V., and Newton, P. (1975) *Ann. NY Acad. Sci.* 258, 243–252.
- Okamura, M. (1979) *J. Nutr. Sci. Vitaminol.* 25, 269.
- Vera, J. C., Rivas, C. I., Fischberg, J., and Golde, D. W. (1993) *Nature* 364, 79–82.
- Wagner, E. S., White, W., Jennings, M., and Bennett, K. (1987) *Biochim. Biophys. Acta* 902, 133–136.
- Bianchi, J., and Rose, R. C. (1986) *Proc. Soc. Exp. Biol. Med.* 181, 333–337.
- Rose, R. C. (1988) *Biochim. Biophys. Acta* 947, 335–366.
- Washko, P. W., Welch, R. W., Dhariwal, K. R., Wang, Y., and Levine, M. (1992) *Anal. Biochem.* 204, 1–14.
- Fabry, M. E., and San George, R. C. (1983) *Biochemistry* 22, 4119–4125.
- Kirk, K., and Kuchel, P. W. (1988) *J. Biol. Chem.* 263, 130–134.
- Kuchel, P. W. (1989) In *Analytical NMR* (Field, L. D., and Sternhell, S., Eds.) pp 157–219, Wiley, London.
- Drew, K. N., Church, T. J., Basu, B., Vuorinen, T., and Serianni, A. S. (1996) *Carbohydr. Res.* 284, 135–143.
- Ohmori, M., and Takagi, M. (1978) *Agric. Biol. Chem.* 42, 173.
- Bubb, W. A., Kirk, K., and Kuchel, P. W. (1988) *J. Magn. Reson.* 77, 363–368.
- Potts, J. R., and Kuchel, P. W. (1992) *Biochem. J.* 281, 753–759.
- Kirk, K., and Kuchel, P. W. (1985) *J. Magn. Reson.* 62, 568–572.
- Kirk, K., and Kuchel, P. W. (1988) *Biochemistry* 27, 8795–8810.
- Kirk, K., Kuchel, P. W., and Labotka, R. J. (1988) *Biophys. J.* 54, 241–247.
- Bianchi, J., and Rose, R. C. (1986) *Toxicology* 40, 75–82.
- Raghoebar, M., Huisman, J. A. M., Van den Berg, W. B., and Van Ginneken, C. A. M. (1987) *Life Sci.* 40, 499–510.
- Winkler, B. (1987) *Biochim. Biophys. Acta* 925, 258–264.
- Meister, A. (1992) *Biochem. Pharmacol.* 44, 1905–1915.
- Raftos, J. E., Kirk, K., and Kuchel, P. W. (1988) *Biochim. Biophys. Acta* 968, 160–166.
- Kuchel, P. W., Chapman, B. E., and Potts, J. (1987) *FEBS Lett.* 219, 5–10.
- Kuchel, P. W. (1989) In *Organised Multienzyme Systems: Catalytic Properties* (Welch, G. R., Ed.) pp 303–380, Academic Press, Orlando.
- Sha'afi, R. I., Rich, S. T., Sidel, V. W., Bossert, W., and Solomon, A. K. (1967) *J. Gen. Physiol.* 50, 1377–1399.
- Xu, A. S. L., and Kuchel, P. W. (1993) *Biochim. Biophys. Acta* 1150, 35–44.
- Sauberlich, H. E., Green, M. B., and Omaye, S. T. (1982) In *Ascorbic Acid: Chemistry, Metabolism, and Uses* (Seib, P. A., and Tolbert, B. M., Eds.) pp 199–221, American Chemical Society, Washington, DC.

38. Seib, P. A., and Tolbert, B. M., Eds. (1982) *Ascorbic Acid: Chemistry, Metabolism and Uses*, American Chemical Society, Washington, DC.
39. Beutler, E. (1984) *Red Cell Metabolism: A Manual of Biochemical Methods*, pp 77–78, Grune and Stratton, Orlando.
40. Benga, G. (1988) *Prog. Mol. Biophys. Mol. Biol.* 51, 193–245.
41. Martensson, J., and Meister, A. (1991) *Proc. Natl. Acad. Sci. U.S.A.* 88, 4656–4660.
42. Levine, M., Morita, K., and Pollard, H. (1985) *J. Biol. Chem.* 260, 12942–12947.
43. Ahn, N. G., and Klinman, J. P. (1987) *J. Biol. Chem.* 262, 1485–1492.
44. Dhariwal, K. R., Washko, P., Hartzell, W. O., and Levine, M. (1989) *J. Biol. Chem.* 264, 15404–15409.
45. Villalba, J. M., Canalejo, A., Barón, M. I., Córdoba, F., and Navas, P. (1993) *Biochem. Biophys. Res. Commun.* 192, 707–713.
46. Zamudio, I., and Canessa, M. (1966) *Biochim. Biophys. Acta* 120, 165–169.
47. Wang, C. S. (1980) *Biochim. Biophys. Acta* 616, 22–29.

BI970765S